Remote Sensing of Smoke, Land and Clouds from the NASA ER-2 during SAFARI 2000

MICHAEL D. KING,[1] STEVEN PLATNICK,[2, 3] CHRISTOPHER C. MOELLER,[4]
HENRY E. REVERCOMB[4] AND D. ALLEN CHU,[5, 3]

Short title: Remote Sensing of Smoke, Land, and Clouds during SAFARI 2000

Journal of Geophysical Research

(Manuscript submitted November 22, 2002)

[1] Earth Sciences Directorate, NASA Goddard Space Flight Center, Greenbelt, Maryland.
[2] Joint Center for Earth Systems Technology, University of Maryland Baltimore County, Baltimore, Maryland.
[3] Laboratory for Atmospheres, NASA Goddard Space Flight Center, Greenbelt, Maryland.
[4] Space Science and Engineering Center, University of Wisconsin-Madison, Madison, Wisconsin.
[5] Science Systems and Applications, Inc., Seabrook, Maryland.

Authors – Dr. Michael D. King
NASA Goddard Space Flight Center
Code 900
Greenbelt, MD 20771
(301) 614-5636
(301) 614-5620 (fax)
king@climate.gsfc.nasa.gov

Dr. Steven Platnick
NASA Goddard Space Flight Center
Code 913
Greenbelt, MD 20771
(301) 614-6243

Mr. Christopher O. Moeller
Cooperative Institute for Meteorological Satellite Studies
University of Wisconsin
Madison, WI 53706-1695
(608) 263-7494

Dr. Henry E. Revercomb
Space Science and Engineering Center
University of Wisconsin
Madison, WI 53706-1695
(608) 263-6758

Dr. D. Allen Chu
NASA Goddard Space Flight Center
Code 913
Greenbelt, MD 20771
(301) 614-6237

Abstract

The NASA ER-2 aircraft was deployed to southern Africa between August 17 and September 25, 2000 as part of the Southern Africa Regional Science Initiative (SAFARI) 2000. This aircraft carried a sophisticated array of multispectral scanners, multiangle spectroradiometers, a monostatic lidar, a gas correlation radiometer, upward and downward spectral flux radiometers, and two metric mapping cameras. These observations were obtained over a 3200 × 2800 km region of savanna, woody savanna, open shrubland, and grassland ecosystems throughout southern Africa, and were quite often coordinated with overflights by NASA's Terra and Landsat 7 satellites. The primary purpose of this sophisticated high altitude observing platform was to obtain independent observations of smoke, clouds, and land surfaces that could be used to check the validity of various remote sensing measurements derived by Earth-orbiting satellites. These include such things as the accuracy of the Moderate Resolution Imaging Spectroradiometer (MODIS) cloud mask for distinguishing clouds and heavy aerosol from land and ocean surfaces, and Terra analyses of cloud optical and microphysical properties, aerosol properties, leaf area index, vegetation index, fire occurrence, carbon monoxide, and surface radiation budget. In addition to coordination with Terra and Landsat 7 satellites, numerous flights were conducted over surface AERONET sites, flux towers in South Africa, Botswana, and Zambia, and in situ aircraft from the University of Washington, South Africa, and the United Kingdom.

1. Introduction

The Southern Africa Regional Science Initiative 2000 (SAFARI 2000) was conducted from August 17 to September 25, 2000 to evaluate the contribution of emissions from biogenic, pyrogenic, and industrial sources to the sub-continental haze over southern Africa. During this time of year, corresponding to the dry season, the regional haze is dominated by transport in a counterclockwise atmosphere gyre over the sub-continent that enhances mixing of industrial pollution, biomass burning aerosol from domestic and grassland fires, and biogenic sources from the soil. This time of year is also a time of frequent and persistent stratocumulus clouds off the coast of Namibia and Angola that form over the nutrient rich, and cold, Benguela Current. These environmental conditions lend themselves to favorable conditions for an assessment of the accuracy of satellite-derived properties of the atmosphere (clouds, aerosols, carbon monoxide, ozone) as well as characteristics of the land surface (leaf area index, fire occurrence, spectral reflectance). As such, observations collected during the experiment provide a unique opportunity for algorithm development teams on the Terra satellite to intercompare satellite-derived surface and atmospheric properties with nearly simultaneous observations obtained from high-altitude aircraft, in situ aircraft, and surface networks of towers and sun/sky radiometers.

The strategy of the SAFARI 2000 experiment was to use research aircraft to obtain remote and in situ measurements of the properties of the atmosphere and surface, with the NASA ER-2 aircraft flying at an altitude of 20 km and serving as a customized satellite with sensors equivalent to those on the Terra [*King and Herring*, 2000] and Aqua spacecraft. Other lower altitude aircraft (University of Washington CV-580, two South African Weather Service Aerocommander 690As, and the United Kingdom C-130H aircraft), were equipped with in situ and re-

mote sensing instruments, and were often coordinated with overflights by Terra as well as the NASA ER-2. Many of the flights were collocated over an extensive network of Aerosol Robotic Network [AERONET; *Holben et al*., 1998] sun/sky radiometers distributed throughout the world, 15 of which were located in southern Africa. Finally, there were 3 highly instrumented towers in Skukuza, South Africa, Maun, Botswana, and Mongu, Zambia that focused a number of aircraft overflights.

The NASA ER-2 aircraft was equipped with eight sensors, the MODIS Airborne Simulator [MAS; *King et al*., 1996], the Cloud Physics Lidar [CPL; *McGill et al*., 2002], the Solar Spectral Flux Radiometer [SSFR; *Pilewskie et al*., 2003], the Airborne Multiangle Imaging Spectroradiometer [AirMISR; *Diner et al*., 1998b], the Measurement of Pollution in the Troposphere-Airborne [MOPITT-A; *Jounot and Drummond*, 2002], the Scanning High-resolution Interferometer Sounder [S-HIS; *Revercomb et al*., 1998], the Leonardo Airborne Simulator [LAS], and a dual RC-10 camera system.

The main objectives of the ER-2 included: (i) collecting MAS data to validate the MODIS cloud mask algorithm for distinguishing clouds and heavy aerosol from land and ocean surfaces, (ii) collecting data for retrieving cloud radiative and microphysical properties over Namibian stratus, (iii) determining the radiative energy budget of savanna, woody savanna, open shrubland, and ocean ecosystems, (iv) determining the vertical distribution of haze layers over southern Africa, (v) comparing high-altitude remote sensing and ground-based observations of surface reflectance and leaf area index, and (vi) comparing remote sensing and in situ estimates of carbon monoxide arising from biomass burning.

The intent of this paper is to present typical results from each of the instruments that obtained measurements onboard the ER-2 during this campaign. We

will highlight results that aid in the interpretation and subsequent validation of the spaceborne observations.

2. Design of the Experiment

Between August 17 and September 25, 2000, the ER-2 aircraft was deployed to southern Africa as part of SAFARI 2000, where it was used for extensive overflights of surface networks, industrial emission and biomass burning sources, clouds off the coast of Namibia, and, in coordination where possible, with satellite ground tracks of the Terra and Landsat 7 satellites.

2.1. Satellite Observations

Terra was launched into polar orbit on December 18, 1999 and acquired its first Earth observations on February 24, 2000. Terra is conducting a comprehensive examination of the land, atmosphere, and ocean surfaces using its five state-of-the-art sensors [*King and Herring*, 2000], and SAFARI 2000 provided a unique opportunity to validate observations obtained by Terra of the southern Africa ecosystem and atmosphere. Terra flies in a 705 km sunsynchronous polar orbit that descends from North to South, crossing the equator at 10:45 local time.

Terra carries 5 sensors with varying spectral and spatial characteristics. Among these are the Moderate Resolution Imaging Spectroradiometer (MODIS), Multi-angle Imaging SpectroRadiometer (MISR), Clouds and the Earth's Radiant Energy System (CERES), Measurements of Pollution in the Troposphere (MOPITT), and Advanced Spaceborne Thermal Emission and Reflection Radiometer (ASTER). Taken together, these sensors are designed to monitor 16 vital signs of the Earth's environment, and in order to verify their accuracies, it is necessary to make observations all over the world and under a wide variety of conditions. To that end, SAFARI 2000 provided a unique opportunity to intercom-

pare satellite observations from Terra with nearly coincident and independent observations of aerosol properties, cloud optical and microphysical properties, surface reflectance, leaf area index, vegetation index, fire occurrence, carbon monoxide, and spectral and broadband radiation flux.

Plate 1 shows an example of cloud and aerosol optical thickness derived from three consecutive daytime orbits of MODIS on September 7, 2000. MODIS has a 2330 km wide swath width and thus small gaps between orbits occur on any given day over the bulk of southern Africa. The true color image in (a) was constructed as a composite of red (0.65 μm), green (0.56 μm), and blue (0.47 μm) bands, which are 3 of the 36 spectral bands carried on this instrument, which range in spatial resolution from 250 m to 1 km, depending on band. The accompanying images show the (b) cloud optical thickness at 0.65 μm and (c) aerosol optical thickness at 0.55 μm. In addition to these parameters, the MODIS atmosphere algorithms include the cloud mask for distinguishing clear sky from clouds, atmospheric profiles of temperature and water vapor, aerosol properties, total precipitable water, cloud properties, and gridded (1° latitude x 1° longitude) time-averaged products at daily, eight-day, and monthly time scales [cf. *King et al*., 2003].

The cloud optical thickness is derived globally at 1 km spatial resolution from a combination of a nonabsorbing wavelength (0.65 μm over land and 0.86 μm over ocean) and a shortwave-infrared absorbing wavelength [*Platnick et al*., 2003], and depends on the MODIS cloud mask and other input to distinguish cloudy pixels from noncloudy or clear pixels. Plate 1b shows the cloud optical thickness derived from both water and ice clouds, and is clearly applied over all cloudy pixels. Marine stratocumulus clouds of optical thicknesses between 10 and 20 are prevalent along the Namibia and Angola coasts. The vast majority of

the African subcontinent is devoid of clouds on this day, a not uncommon occurrence during the dry season, with more cloudiness occurring in the Mozambique lowlands.

The aerosol optical thickness is retrieved using different algorithms over the ocean [*Tanré et al*., 1997] and land [*Kaufman et al*., 1997], with both algorithms matching the multispectral reflectance observations to lookup tables of precomputed reflectances. These algorithms have recently been updated as described by *King et al.* [2003] so that more frequent retrievals are made over bright deserts and additional tests are applied for cloud screening over ocean. Although this product is produced globally on a 10 km grid, the algorithm is applied to the darkest cloud-free pixels in each 10 km region, and excludes analysis in sunglint regions over the ocean. Plate 1c shows that the bulk of the aerosol load is in northern Botswana, Zambia, Angola, southern Mozambique, and northern Namibia. Due to strong outflow of absorbing aerosol from Angola over the boundary layer stratus clouds along the coast, there is some false detection of aerosol layers in the column that also contains clouds. Experiments such as SAFARI 2000 permit an intercomparison of the aerosol retrievals from MODIS and MISR on Terra with the NASA ER-2 as well as ground-based sunphotometers from AERONET. Intercomparison of these results from MISR during SAFARI 2000 can be found in *Diner et al*. [2001] and from MODIS over a wide variety of land surfaces in *Chu et al*. [2002].

In addition to Terra, the Landsat 7 satellite is in orbit at the same altitude and on the same ground track as Terra but only 40 minutes earlier. Hence, on numerous occasions, the NASA ER-2 aircraft was coordinated with Landsat 7's high spatial resolution imagery as well as Terra's moderate spatial resolution and wide swath observations. The ASTER instrument on Terra is, in many respects,

comparable to Landsat's Enhanced Thematic Mapper Plus (ETM+) sensor, but with more thermal infrared and shortwave infrared bands (and a narrower swath). However, ASTER needs to be scheduled to acquire observations, as it only has an 8% duty cycle, so the data from ASTER are more sparse in coverage than those of other spaceborne sensors, including Landsat's ETM+, during SAFARI 2000.

2.2. Surface Observations

An extensive network of ground-based sun/sky radiometers are deployed throughout the world as part of the AERONET program. Of the ~120 identical globally distributed Cimel sun/sky radiometers, 15 were distributed throughout southern Africa as part of SAFARI 2000 dry season campaign (cf. Plate 2). These radiometers are used, together with a sophisticated instrument maintenance, calibration, cloud screening, and data processing system [*Holben et al.*, 1998; *Smirnov et al.*, 2000], to derive aerosol optical thickness, aerosol size distribution, and single scattering albedo using a new AERONET inversion algorithm [*Dubovik and King*, 2000].

Since both the MISR and MODIS instruments onboard Terra have extraordinary capability for deriving aerosol optical thickness and size parameters over both land and ocean, many satellite intercomparisons were made with these AERONET sites [*Diner et al.*, 2001; *Chu et al.*, 2002]. In addition, many aircraft flights, both with the ER-2 as well as with the other research aircraft used during SAFARI 2000 (University of Washington CV-580 and two South African Weather Service Aerocommander 690As, known as JRA and JRB) overflew the AERONET sites during SAFARI 2000.

There were 3 highly instrumented towers operating during SAFARI 2000 at Skukuza, South Africa, Maun, Botswana, and Mongu, Zambia, the locations of

which are shown in Plate 2. In addition to the measurement suite on these flux towers [*Scholes et al*., 2001; *Otter et al*., 2002], there were surface micropulse lidars operating at Skukuza and Mongu [*Campbell et al.*, 2003] and the Surface Measurements for Atmospheric Radiative Transfer (SMART) system at Skukuza.

Finally, as part of the strategy of SAFARI 2000, aircraft (and satellite) overflights occurred over various industrial locations, including the coal fired power plants at Witbank, South Africa, gold mines around Francistown and Selebi-Phikwe, Botswana, and the copper mines at Phalaborwa. These industrial locations are shown in Plate 2 and were overflown on numerous occasions, along with other industrial locations in South Africa, Botswana, and Zambia.

2.3. ER-2 Observations

The NASA ER-2 high-altitude research aircraft provided multispectral and multiangle imagery as well as vertical profiles of clouds and aerosols during SAFARI 2000. This aircraft was used as a dedicated remote sensing platform that was coordinated with satellite observations from Terra, Landsat 7, and Earth Probe TOMS (Total Ozone Mapping Spectrometer) during their respective overpass times and orbits, and which then overflew numerous ground-based sites, industrial locations, prescribed burns, and regional haze and clouds.

Table 1 summarizes the instruments onboard the ER-2 aircraft during SAFARI 2000, which included airborne simulators for MODIS, MISR, and MOPITT, a vertically profiling lidar (CPL), a scanning Michelson interferometer (S-HIS), a hyperspectral imager (LAS), an upward- and downward-looking spectral flux radiometer (SSFR), and twin metric mapping cameras (RC-10). From the nominal ER-2 altitude of 20 km, the swath width and pixel size varied considerably between these instruments. MOPITT-A and CPL were nadir instruments only, SSFR was a spectral flux radiometer with a cosine-weighted integral of

downwelling and upwelling radiation, and all other instruments either scanned or had a cross track imaging capability. The cameras, though pointed towards nadir, produced photographs that were 13 km in width, centered on nadir.

During August and September 2000, the NASA ER-2 aircraft conducted 18 research flights throughout southern Africa. Plate 3 shows the coverage of three of the ER-2 sensors during the SAFARI 2000 dry season campaign, where the MAS had the widest swath width (37 km) and operated once the aircraft reached its cruising altitude and until the start of its descent. The RC-10 metric mapping cameras were operated only for specific measurement objectives, and were turned on at predetermined locations during the flight. Finally, AirMISR had a targeted acquisition strategy that required straight and level flight for a period of time so that the camera could be rotated in sequence over the 9 look angles of MISR. Due to technical difficulties, AirMISR operated the most during the latter half of the experiment. A careful examination of the ground tracks in Plate 3 shows the numerous times in which the ER-2 flew in a SSW-NNE orientation closely aligned with the Terra and Landsat 7 ground tracks.

Table 2 summarizes the measurement objectives and primary aircraft, satellite, and surface coordination for all 18 ER-2 research flights. Almost every flight was coordinated with the Terra and Landsat satellites and on four occasions there was some coordination with the Earth Probe TOMS spacecraft. Flights were conducted over 8 countries throughout southern Africa, with an especially high concentration over Kruger National Park and the Skukuza Tower site in South Africa as well as numerous flights over the Western Province of Zambia and the Mongu airport and tower location. For the entire mission, the base of operations for the ER-2 was Polokwane (formerly Pietersburg), South Africa, which led to long flights for the latter portion of the experiment that took the air-

craft over the Namib Desert, Etosha Pan, and the stratocumulus clouds off Namibia and Angola. One flight was conducted at night and was focused on the numerous fires in western Zambia.

3. Results from Observations

In order to validate remote sensing observations from the Terra spacecraft, the ER-2 overflew a wide variety of surface sites, emission sources, and clouds. In this section we will present some examples of data collected during SAFARI 2000 that illustrate the technology used in the experiment and how these data can be synthesized and integrated to help verify the accuracy and utility of satellite observations.

3.1. AirMISR

The Airborne Multi-angle Imaging SpectroRadiometer (AirMISR) instrument was developed to assist in validation of the MISR experiment onboard Terra [*Diner et al*., 1998a]. Unlike MISR, which contains nine individual cameras pointed at discrete look angles, AirMISR utilizes a single camera in a pivoting gimbal mount. Because AirMISR was fabricated from MISR brassboard and engineering model components, it has a similar radiometric and spectral response and the same spectral characteristics as the MISR cameras.

Due to power supply problems, AirMISR operated on only 4 of 18 flights during SAFARI 2000. One of these missions was September 7, 2000, when the ER-2 was coordinated with the Terra spacecraft over the Timbavati Private Game Reserve outside Kruger National Park, South Africa. The ER-2 made 3 passes over a prescribed burn, the first of which coincided with the Terra overpass. Plate 4a shows an 85 × 200 km swath of MISR's aft-viewing 45° camera and Plate 4b a smaller (9 × 9 km), more detailed, AirMISR view from its nadir view. The

larger MISR view shows not only the fires from the Timbavati controlled burn, but also some burn scars from previous fires. At the lower left are the Drakensburg Mountains. Time series from AirMISR (and other sensors onboard the ER-2) show the rapid expansion of the burn scar as the fire burned over the 45 minutes that the ER-2 continued to overfly the region. MODIS was used to derive the fire location and burn scar area, and these results were compared with the higher resolution observations from the AirMISR (and MAS) on the ER-2.

3.2. S-HIS

The Scanning High-resolution Interferometer Sounder (S-HIS) is a Fourier-transform interferometer that covers the spectral range 3.3-16.7 μm. It scans cross track with 11 Earth-viewing pixels per scan at a scan rate of 15 s per scan, resulting in multispectral images 36 km in width with a spatial resolution of 2 km at nadir. One of the key elements of S-HIS is its better than 0.5°C radiometric accuracy.

Plate 5 shows an example of S-HIS observations of the 10.2 μm brightness temperature acquired over the Okavango Delta, Botswana, during 6 parallel flight lines on August 27, 2000. The Okavango Delta is the largest inland Delta in the world, and is at its highest water level in August and September when the rest of southern Africa is quite dry. As a consequence, it is quite a magnate for birds and animals at that time of year. Plate 5 shows that the water temperature in the Delta is 299-303 K, in contrast to temperatures in excess of 310 K in the eastern half of the Delta, an area that includes the Maun Tower. Note also that the brightness temperature is higher along the nadir than towards the limb of each flight line, a direct consequence of water vapor in the atmospheric column.

S-HIS also revealed a unique feature of high-resolution infrared spectra associated with fires. Plate 4c includes a shortwave band spectrum from the over-

pass of the prescribed fire in the Timbavati Game Reserve that contains an unusual sharp spike at the 2400 cm^{-1} CO_2 band head. This fire signature was an unanticipated finding of SAFARI 2000, although this type of feature is well known in association with hot jet or rocket engine exhaust. In this context it has been named the 'blue spike' because of its appearance on the short wavelength side of the 4.3 μm CO_2 band. Normal upwelling brightness temperature spectra at S-HIS resolution display a monotonic increase with wavenumber in this region, shaped by a combination of CO_2 line structure and the nitrogen continuum. The blue spike for fires requires the advection of air heated by the fire over a cooler surface. For the relatively large S-HIS footprint of 2 km, this situation is well represented inside each footprint in which the active fire is just a narrow line. The spectroscopy associated with this fire feature is the strong temperature dependence of line strengths for high-J lines at the shortwave edge of the band. Line strength increases lead to an effective band broadening for the hot gas layer that allows its emission to escape absorption by the CO_2 in overlying layers. We expect this spectral feature to be a useful tool in future remote sensing characterization of fires.

3.3. MAS

The MODIS Airborne Simulator (MAS) is a cross-track scanning spectrometer that measures reflected solar and emitted thermal radiation in 50 narrowband channels. For the SAFARI 2000 deployment, the configuration of the MAS contained channels between 0.47 and 14.2 μm. At a nominal ER-2 altitude of 20 km, the MAS images a swath width of 37.2 km centered on the aircraft ground track, with a total of 716 Earth-viewing pixels acquired per scan with the nadir-most pixel having a spatial resolution of 50 m.

Some of these bands are used to discriminate clouds from clear sky (cloud

mask) where others are used to derive the optical and microphysical properties of clouds and aerosols, and others used to derive surface reflectance, leaf area index, burn scars, and fire energy. Plate 6 shows multispectral images of a scene acquired over a controlled burn in Madikwe Private Game Reserve, South Africa. These images were resampled at a constant spatial resolution to remove distortion of surface features near the edge of the swath. The uppermost image is a true color composite constructed from the 0.66, 0.55, and 0.47 μm bands, and shows smoke associated with a prescribed fire along a road in the lower portion of the image. Also evident in the upper right portion of the image is a low-level cloud and its corresponding shadow. The middle image is a false color composite of bands at 3.94, 2.18, and 1.67 μm. With these shortwave infrared bands, the hot fire line beneath the smoke is clearly evident, as is the hot ground of a recent burn scar along the right-hand edge of the scene. The burn scar is hard to distinguish from a shadow in the upper image, but is clearly warm and therefore a result of recent burning. These images were acquired as the ER-2 aircraft flew in a northerly direction (6.4° heading) when the solar zenith angle was 43°. With the sun to the north in the Southern Hemisphere, the cloud shadow is on the southern portion of the cloud.

The cloud mask algorithm uses 10 of the available 50 spectral bands available on MAS to distinguish clear sky from clouds, identify heavy aerosol, and determine pixels contaminated by cloud shadow and fire [cf. *King et al.*, 1998 for details]. Plate 6c represents the results of the cloud, shadow, and fire mask applied to this scene. The cloud mask assigns four levels of clear sky 'confidence' to each pixel. In this panel, the high confidence clear sky image on which the cloud, shadow, and fire masks are superimposed is the MAS reflectance at 0.66 μm. The cloud mask results are designated as cloudy, probably cloudy, probably

clear, and confident clear, with the cloud shadow tests being applied whenever a highly confident clear sky pixel is identified. A cloud shadow is identified when $R_{0.95} < 0.12$, $0.9 < R_{0.87}/R_{0.66} < 1.38$, *and* $T_{3.8} - T_{11} < 6.5$ K, where the last test was incorporated so as to eliminate any pixels containing warm burn scars that are otherwise falsely identified as cloud shadow. Hot fires are identified when $T_{3.8} > 350$ K *and* $T_{3.8} - T_{11} > 10$ K.

Comparing the cloud, shadow, and fire mask results to the true and false color images in the upper two panels of Plate 6, it appears that the clouds and shadows in the vast majority of the image are being classified quite accurately, and the intense fire line near the highway in the middle of the image has been identified without apparent error. The probably clear pixels occur primarily at the very edge of the relatively thin clouds on the left-hand portion of the scene. There is some false detection of high confidence cloud in the vicinity of the heavy aerosol associated with the smoke. Although these false detections do occur, they are relatively rare.

3.4. CPL

The Cloud Physics Lidar (CPL) is a nadir-viewing, monostatic lidar system that provides cloud and aerosol boundaries, vertical structure, and aerosol extinction profiles. SAFARI 2000 was the maiden mission of CPL, which operated well throughout the experiment. The CPL uses a Nd:YAG laser transmitting at 0.532 and 1.064 μm, and the data were averaged over several pulses to provide higher quality vertical extinction density observations at 200 m horizontal and 30 m vertical sampling resolution. This permits the construction of detailed cloud and boundary layer aerosol vertical distributions in the nadir direction, including aerosol extinction profiles and integrated aerosol optical thickness [*McGill et al.*, 2003].

Plate 7 shows CPL observations of attenuated backscatter coefficient on August 24, 2000 obtained at 1.064 μm along the nadir track of the ER-2 as it flew from the highveld west of Witbank, South Africa to the Drakensburg escarpment and Inhaca Island, Mozambique, where the ER-2 turned north over nearby Maputo Bay paralleling the Terra ground track. These data show that the aerosol haze layer over the highveld (0-300 km) was confined below a temperature inversion at ~4 km. Over the lowveld and coastal Mozambique, a second, marine, boundary layer haze was confined below ~2 km, with a well defined 'clear air slot' between them at ~2.5 km in altitude, a phenomenon often observed during SAFARI 2000 and described by *Hobbs* [2002]. Also evident in this figure are aerosol plumes at ~110 km that coincide with flights over the coal fired power plants of Witbank, as confirmed by examination of coincident MAS imagery onboard the ER-2 aircraft. The ER-2 turned between 460 and 470 km to a NNE orientation over Maputo Bay, where it encountered cumulus humilus clouds at ~590-660 km that were confined below ~1 km in altitude.

3.5. SSFR

The Solar Spectral Flux Radiometer (SSFR) is a spectral flux radiometer with a hemispheric field-of-view that measures spectral flux (irradiance) from 0.3-1.7 μm with a spectral resolution of 8-12 nm. Dual SSFRs were integrated on the ER-2 aircraft, one looking upward and one looking downward. This enabled measurements of the spectral downwelling and upwelling irradiance at aircraft altitude, and via the ratio of the two, the spectral albedo of the underlying Earth-atmosphere system.

Plate 8 illustrates the upwelling and downwelling spectral fluxes obtained at four different times and locations on August 24, 2000. On this flight, which overflew coastal Mozambique, three of the observations were obtained over land sur-

faces while the observations at 8.195 UTC were obtained over Inhaca Island and nearby water of Maputo Bay. The lower panel shows the spectral albedo derived from the ratio of upwelling to downwelling flux, and clearly shows reflectance by atmospheric gases and aerosols at wavelengths less than about 400 nm, enhanced spectral reflectance of the land surfaces relative to water surfaces for wavelengths greater than 700 nm, strong water vapor absorption bands at 940, 1125, and 1400 nm, and oxygen absorption bands at 690 and 760 nm. Land surfaces are noticeably brighter in the near- and shortwave-infrared region than at visible wavelengths, and water bodies are noticeably darker. The ER-2 flies above ~95% of the Earth's atmosphere, so the SSFR on the ER-2 records spectral reflectance close to what a satellite would observe outside the Earth's atmosphere.

3.6. MOPITT-A

MOPITT-A is the aircraft version of the Terra Measurements Of Pollution In The Troposphere (MOPITT) instrument [*Drummond and Mand*, 1996]. It was completed shortly before the ER-2 deployment to SAFARI 2000. The instrument is a four-channel correlation radiometer operating at 4.7 and 2.2 μm to measure carbon monoxide and methane in the lower atmosphere. Based on the MOPITT engineering model, it shares the same angular field-of-view that, combined with the ER-2 flight altitude and the four pixels of the MOPITT detector array, gave an overall coverage of 630 m along track × 2520 m cross track on the ground.

Plate 9 shows the radiance along the aircraft track below the MOPITT-A instrument taken on September 7, 2000. This flight had two objectives: to overfly the Timbavati bush fire, and to underfly the MOPITT instrument on Terra over the ocean. The colors indicate the 4.7 μm emitted radiance in units of W m^{-2} sr^{-1}. This radiance is indicative of ground or cloud-top temperature in the underlying

scene.

3.7. LAS

The Leonardo Airborne Simulator (LAS) represents a new class of hyperspectral imagers that use non-dispersive thin film filters as wavelength selective elements (e.g., a wedged filter of linear variable etalon). The LAS has no moving parts, minimal optical elements, and only one electronically activated element, the detector array (1024 × 1024 Indium Antimonide, InSb, detectors). Operating in a pushbroom mode, LAS obtains a 3-D data cube by scanning the image of a surface over the focal plane (one axis of the array for spectral and the other for spatial sampling). The scanning motion is provided by the aircraft motion. For the SAFARI 2000 deployment, the LAS performed an engineering mission, utilizing only a single wavelength at 2.1 μm with a 13.5^o field-of-view (FOV) optical lens, due to delays in delivering the wedged filter (0.4-2.5 μm) and the wide field of view (80^o) refractive module. Hence, no science data were acquired on this, its maiden, mission.

3.8. RC-10 Cameras

The ER-2 carried dual RC-10 cameras in the Q-Bay, with one having color infrared film and the other black and white film. Using a 304.67 mm f/4.0 lens, the spatial coverage of each photograph is 13 km in swath width with pixel sizes ranging from 1.5 m at nadir to 7.6 m at the edge of the frame. Each camera has a film capacity of 122 m of film, and enabled targeted acquisitions of high spatial resolution photography to be acquired throughout the deployment (cf. Plate 2). During SAFARI 2000, 3397 frames of color infrared film were acquired, of which 1333 were in South Africa, 714 in Namibia, 444 in Botswana, 443 in Zambia, 430 in Mozambique, and 33 in Malawi.

Plate 10 shows a color infrared photograph of Mongu, Zambia, acquired on August 25, 2000. This location includes the Mongu airport to the northeast of town (left-hand middle part of the photograph), where the micro-pulse lidar network [*Campbell et al.*, 2003] was operated. To the west of town is the Zambezi River floodplain, which is largely dry in August and September with seasonal flooding during the wet season. The Mongu Tower is located 20 km southeast of Mongu in the Kataba Forest Reserve, and is outside the field of view of this photograph.

4. Summary and Conclusions

The SAFARI 2000 dry season campaign was conducted during August and September 2000 with a goal of studying the southern African earth-atmosphere-human system with a special emphasis on the biogenic, pyrogenic, and anthropogenic aerosol and trace gas emissions in the region [cf. *Swap et al.*, 2002]. The overall design of the experiment consisted of combining measurements from the surface, research aircraft, and satellites, to explore the properties of the atmosphere and ecology during the dry season in southern Africa. During the course of the SAFARI 2000 campaign, multi-aircraft overflights were obtained over AERONET sites, flux towers, industrial and mining locations, and a broad range of clouds and ecosystems. Many of these flights were coordinated with nearly simultaneous overflights of NASA's Terra, Landsat 7, and Earth Probe TOMS satellites. As part of this experiment, the NASA ER-2 aircraft carried a sophisticated array of multispectral scanners, multiangle spectroradiometers, a monostatic lidar, a gas correlation radiometer, upward and downward spectral flux radiometers, and two metric mapping cameras. This platform acquired observations over a vast area of southern Africa that included major portions of eight countries.

Preliminary analysis of the data from the ER-2 indicates that the dataset contains a wealth of information on clouds, aerosols, tropospheric chemistry, surface reflectance, land and sea surface temperature, and radiation. Preliminary scientific highlights from each of the sensors onboard the ER-2 have been presented in this paper and, for the most part, these data are already available to the wider scientific community to pursue further analysis.

Acknowledgments. This study was part of the Southern Africa Regional Science Initiative (SAFARI 2000), and was supported by the EOS Project Science Office. SP was supported by NASA Grant NAG5-6996 to the University of Maryland Baltimore County, COM by NASA Grant NAS1-99106 to the University of Wisconsin-Madison, HER by NASA Grant NAS5-11155 and Integrated Program Office (IPO) contract number 50-SPNA-1-00039 to the University of Wisconsin-Madison, and DAC by NASA Grant NAS5-31366 to Science Systems and Applications, Inc. We would like to express our appreciation to D. J. Diner, J. S. Myers, M. J. McGill, P. Pilewskie, and J. R. Drummond for providing data used in this paper, and J. Riédi, W. H. Humberson, R. T. Dominguez for providing graphics and visualization support for Plates 2 and 3. The coordination of multiple aircraft and satellite observations, with due attention to the international agreements and meteorological conditions, were greatly aided with the special assistance of J. T. Suttles, R. J. Swap, and H. J. Annegarn.

References

Ackerman, S. A., K. I. Strabala, W. P. Menzel, R. A. Frey, C. C. Moeller, and L. E. Gumley, Discriminating clear-sky from clouds with MODIS, *J. Geophys. Res.*, *103*, 32141-32158, 1998.

Campbell, J. R., E. J. Welton, J. D. Spinhirne, Q. Ji, S. C. Tsay, S. J. Piketh, M.

Barenbrug, and B. N. Holben, Micropulse lidar observations of tropospheric aerosols over northeastern South Africa during ARREX and SAFARI-2000 dry season experiments, *J. Geophys. Res*., this issue, 2003.

Chu. D. A., Y. J. Kaufman, C. Ichoku, L. A. Remer, D. Tanré, and B. N. Holben, Validation of MODIS aerosol optical depth retrieval over land, *Geophys. Res. Lett*., *29(12)*, DOI 10.1029/2001GL013205, 2002.

Diner, D., J. Beckert, T. Reilly, C. Bruegge, J. Conel, R. Kahn, J. Martonchik, T. Ackerman, R. Davies, S. Gerstl, H. Gordon, J. P. Muller, R. Myneni, P. Sellers, B. Pinty, and M. Verstraete, Multi-angle Imaging SpectroRadiometer instrument description and experiment overview, *IEEE Trans. Geosci. Remote Sens.*, *36*, 1072-1087, 1998a.

Diner, D. J., L. M. Barge, C. J. Bruegge, T. G. Chrien, J. E. Conel, M. L. Eastwood, J. D. Garcia, M. A. Hernandez, C. G. Kurzweil, W. C. Ledeboer, N. D. Pignatano, C. M. Sarture, and B. G. Smith, The Airborne Multi-angle Imaging SpectroRadiometer (AirMISR): Instrument description and first results, *IEEE Trans. Geosci. Remote Sens.*, *36*, 1339-1349, 1998b.

Diner, D. J., W. A. Abdou, C. J. Bruegge, J. E. Conel, K. A. Crean, B. J. Gaitley, M. C. Helmlinger, R. A. Kahn, J. V. Martonchik, S. H. Pilorz, and B. N. Holben, MISR aerosol optical depth retrievals over southern Africa during the SAFARI-2000 dry season campaign, *Geophys. Res. Lett.*, *28*, 3127-3130, 2001.

Drummond, J. R., and G. S. Mand, The measurements of pollution in the troposphere (MOPITT) instrument: Overall performance and calibration requirements, *J. Atmos. Oceanic Technol.*, *13*, 314-320, 1996.

Dubovik, O., and M. D. King, A flexible inversion algorithm for retrieval of aerosol optical properties from sun and sky radiance measurements, *J. Geophys. Res*., *105*, 20673-20696, 2000.

Hobbs, P. V., Clean air slots amid atmospheric pollution, *Nature*, *415*, 861.

Holben, B. N., T. F. Eck, I. Slutsker, D. Tanré, J. P. Buis, A. Setzer, E. Vermote, J. A. Reagan, Y. J. Kaufman, T. Nakajima, F. Lavenu, I. Jankowiak, and A. Smirnov, AERONET—A federated instrument network and data archive for aerosol characterization, *Remote Sens. Environ.*, *66*, 1-16, 1998.

Jounot, L. J., and J. R. Drummond, Measurements of Pollution in the Troposphere–Airborne (MOPITT-A), *Proc. Inter. Geosci. Remote Sens. Symp.*, Toronto, Canada, 2002.

Kaufman, Y. J., D. Tanré, L. A. Remer, E. F. Vermote, A. Chu, and B. N. Holben, Operational remote sensing of tropospheric aerosol over land from EOS Moderate Resolution Imaging Spectroradiometer, *J. Geophys. Res.*, *102*, 17051-17067, 1997.

King, M. D., and D. D. Herring, Monitoring Earth's vital signs, *Sci. Amer.*, *282*, 72–77, 2000.

King, M. D., S. C. Tsay, S. A. Ackerman and N. F. Larsen, Discriminating heavy aerosol, clouds, and fires during SCAR-B: Application of airborne multispectral MAS data, *J. Geophys. Res.*, *103*, 31989-31999, 1998.

King, M. D., W. P. Menzel, P. S. Grant, J. S. Myers, G. T. Arnold, S. E. Platnick, L. E. Gumley, S. C. Tsay, C. C. Moeller, M. Fitzgerald, K. S. Brown, and F. G. Osterwisch, Airborne scanning spectrometer for remote sensing of cloud, aerosol, water vapor and surface properties, *J. Atmos. Oceanic Technol.*, *13*, 777-794, 1996.

King, M. D., W. P. Menzel, Y. J. Kaufman, D. Tanré, B. C. Gao, S. Platnick, S. A. Ackerman, L. A. Remer, R. Pincus, and P. A. Hubanks, Cloud and aerosol properties, precipitable water, and profiles of temperature and humidity from MODIS, *IEEE Trans. Geosci. Remote Sens.*, in press, 2003.

McGill, M. J., D. L. Hlavka, W. D. Hart, V. S. Scott, J. D. Spinhirne, and B. Schmid, Cloud Physics Lidar: Instrument description and initial measurement results, *Appl. Opt.*, *41*, 3725-3734, 2002.

McGill, M. J., D. L. Hlavka, W. D. Hart, E. J. Welton, and J. R. Campbell, Airborne lidar measurements of aerosol optical properties during SAFARI-2000, *J. Geophys. Res.,* this issue, 2003.

Otter, L. B., R. J. Scholes, P. Dowty, J. L. Privette, K. Caylor, S. Ringrose, M. Mukelabai, P. Frost, O. Totolo, and E. M. Veenendaal, The SAFARI 2000 wet season campaigns, *S. African J. Sci.*, *98*, 131-137, 2002.

Pilewskie, P., J. Pommier, R. Bergstrom, W. Gore, S. Howard, M. Rabette and B. Schmid, Solar spectral radiative forcing during the Southern African Regional Science Initiative, *J. Geophys. Res.*, this issue, 2003.

Platnick, S., M. D. King, S. A. Ackerman, W. P. Menzel, B. A. Baum, J. C. Riédi, and R. A. Frey, The MODIS cloud products: Algorithms and examples from Terra, *IEEE Trans. Geosci. Remote Sens.*, in press, 2003.

Revercomb, H. E., V. P. Walden, D. C. Tobin, J. Anderson, F. A. Best, N. C. Ciganovich, R. G. Dedecker, T. Dirkx, S. C. Ellington, R. K. Garcia, R. Herbsleb, R. O Knuteson, D. LaPorte, D. McRae, and M. Werner, Recent results from two new aircraft-based Fourier transform interferometers: The Scanning High-resolution Interferometer Sounder and the NPOESS Atmospheric Sounder Testbed Interferometer, *Proc. 8th Inter. Workshop Atmos. Sci. from Space using Fourier Transf. Spectrom.,* Toulouse, France, 1998.

Scholes, R. J., N. Gureja, M. Giannecchinni, D. Dovie, B. Wilson, N. Davidson, K. Piggot, C. McLoughlin, K. Van der Velde, A. Freeman, S. Bradley, R. Smart, and S. Ndala, The environment and vegetation of the flux measurement site near Skukuza, Kruger National Park, *Koedoe*, *44*, 73-83, 2001.

Smirnov, A., B. N. Holben, T. F. Eck, O. Dubovik, and I. Slutsker, Cloud screening and quality control algorithms for the AERONET data base, *Remote Sens. Environ.*, *73*, 337-349, 2000.

Swap, R. J., H. J. Annegarn, J. T. Suttles, J. Haywood, M. C. Helmlinger, C. Hely, P. V. Hobbs, B. N. Holben, J. Ji, M. D. King, T. Landmann, W. Maenhaut, L. Otter, B. Pak, S. J. Piketh, S. Platnick, J. Privette, D. Roy, A. M. Thompson, D. Ward, and R. Yokelson, The southern African regional science initiative (SAFARI 2000): Overview of the dry season field campaign, *S. African J. Sci.*, *98*, 125-130, 2002.

Tanré, D., Y. J. Kaufman, M. Herman, and S. Mattoo, Remote sensing of aerosol properties over oceans using the MODIS/EOS spectral radiances, *J. Geophys. Res.*, *102*, 16971-16988, 1997.

Table 1. NASA ER-2 Instrumentation, Spectral Coverage, Swath Width, Pixel Size and Data Products, Assuming a Typical Aircraft Flight Level (20 km).

Sensor	Wavelengths	Scanning Mode	Pixel Size	Data Products
MODIS Airborne Simulator (MAS)	0.47-14.2 μm 50 bands	cross track	50 m 37 km swath	solar spectral radiance bidirectional reflectance cloud mask, optical thickness and effective radius aerosol optical thickness
Cloud Physics Lidar (CPL)	1064, 532 nm	nadir	30 m vertical 200 m horizontal	cloud and aerosol boundaries vertical structure aerosol optical thickness aerosol extinction profile
Solar Spectral Flux Radiometer (SSFR)	0.3-1.7 μm 8-12 nm resolution	zenith, nadir		spectral irradiance (downwelling & upwelling) spectral albedo
Airborne Multi-angle Imaging SpectroRadiometer (AirMISR)	446, 558, 672, 866 nm	nine look angles	6 m 9 km swath	georectified top-of-atmosphere bidirectional radiance
Measurement of Pollution in the Troposphere-Airborne (MOPITT-A)	4.7 and 2.2 μm	nadir	0.6 × 2.5 km	carbon monoxide profile
Scanning High Resolution Interferometer Sounder (S-HIS)	3.3-16.7 μm 0.5 cm^{-1} resolution	cross track	2 km 36 km swath	temperature and water vapor profiles surface emissivity column CO
Leonardo Airborne Simulator (LAS)	0.4-2.5 μm 1028 bands	cross track	5 m 6.3 km swath (engineering test)	hyperspectral imagery
Dual RC-10 Camera System	color IR film black & white film	nadir	1.5 m 13 km swath	high resolution metric stereo photography

Table 2. Summary of ER-2 Flights During SAFARI 2000, Together with a Description of Aircraft, Satellite, and Surface Coordination that Occurred During these Flights, and the Primary Purpose of the Mission

Date	Aircraft Coordination	Satellite Coordination	Surface Coordination	Primary Purpose
Aug. 17	JRB	Terra Landsat 7	Skukuza	overflight of Skukuza SMART site and underflight of Terra over the Mozambique Channel for MOPITT validation
Aug. 20	JRA JRB	Terra Landsat 7	–	overflight of Madikwe prescribed fire and underflight of Terra over Madikwe (JRA) and Selibe-Phikwe (JRB)
Aug. 22	CV-580 JRA JRB	Terra Landsat 7	Skukuza	overflight of Durnacol coal mines, Witbank power stations, Johannesburg, Pretoria, and Rustenburg platinum mines; overflew Skukuza SMART site and underflew Terra; coordinated with CV-580 (Skukuza), JRA (Satara prescribed fire), JRB (Johannesburg, Rustenburg, and Witbank)
Aug. 24	CV-580 JRA	Terra Landsat 7	Inhaca Island	overflight of Inhaca Island and underflight of Terra through Mozambique and Malawi; overflight of geologic feature of northern Kruger National Park
Aug. 25	–	Terra Landsat 7	Sua Pan Kaoma Zambezi Mongu Senanga Maun	overflight of Kaoma prescribed burn and underflight of Terra; overflight of AERONET sunphotometer sites at Sua Pan, Kaoma, Zambezi, Mongu airport, Senanga, and Maun Tower
Aug. 27	–	Terra Landsat 7	Sua Pan Maun	overflight of Sua Pan during Terra overpass; overflight of Maun Tower, Okavango Delta, and Kalahari transect sites at Okwa River and Tshane
Aug. 29	–	Terra Landsat 7 EP TOMS	Skukuza	overflight of Skukuza during TOMS overpass; overflight of Witbank, Pilansberg, Messina copper mine, Venetia diamond mine, and geological formations from Phalaborwa to Madikwe
Sept. 1	–	Terra Landsat 7	Mongu	night flight over fires in Zambia; Terra (21:15 UTC) in clear scenes on return
Sept. 4	–	EP TOMS	Sua Pan Maun	AirMISR mapping of Sua Pan; Maun, Okwa River and Tshane

Table 2. Summary of ER-2 Flights During SAFARI 2000 (continued)

Date	Aircraft Coordination	Satellite Coordination	Surface Coordination	Primary Purpose
Sept. 6	CV-580	–	Mongu	Mongu Tower and airfield overflights with CV-580 doing BRDF (tower) and profiling (airfield); prescribed fire at Kaoma
Sept. 7	CV-580	Terra Landsat 7 EP TOMS	Skukuza	Timbavati controlled burn with CV-580 sampling plume and Terra overpass; Skukuza overflight and TOMS line; aged smoke plume scenes from Timbavati fire
Sept. 11	CV-580 C-130Q	Terra Landsat 7	–	first flight to the Namibian coast; stratus along northern coast; overpass of Walvis Bay and Kuiseb River Canyon
Sept. 13	CV-580 C-130Q	Terra Landsat 7	Etosha Pan	stratus along the Namibian coast north to the Angolan border, 3 overpasses of Etosha Pan
Sept. 14	C-130Q	Terra Landsat 7 EP TOMS	–	flight to Angolan stratus, overpass of Brandenberg area and southern Etosha National Park
Sept. 17	JRA	Terra Landsat 7	Maun	Maun tower site, burn scar in NE Namibia, power plants & industrial sites near Johannesburg
Sept. 21	–	Terra Landsat 7	–	Mozambique Channel stratocumulus off Beira
Sept. 23		Terra Landsat 7	Skukuza	Skukuza tower, Malibamatso River Catchment
Sept. 25		Terra Landsat 7	Inhaca Island Skukuza	Mozambique run, over land under Terra overpass, back over water; Inhaca Island, Skukuza tower

PLATE LEGENDS

Plate 1. MODIS atmospheric properties over southern Africa on 3 consecutive descending daytime orbits on September 7, 2000. Panel (a) is a true color composite constructed from red (0.65 μm), green (0.56 μm) and blue (0.47 μm) bands. Panel (b) is the cloud optical thickness at 0.65 μm and (c) the aerosol optical thickness at 0.56 μm.

Plate 2. Location of AERONET, Flux Tower, and primary industrial sites throughout southern Africa that were overflown by the NASA ER-2 aircraft during SAFARI 2000.

Plate 3. Coverage of the RC-10 camera, AirMISR, and MAS on all ER-2 flights throughout SAFARI 2000.

Plate 4. These images of northeastern South Africa were acquired on September 7, 2000 at 0825 UTC by MISR (a) and AirMISR (b). Panel (a) is an 85 x 200 km swath of MISR's aft-viewing 45° camera, and (b) an AirMISR 9 x 9 km nadir-viewing image of the prescribed fire in the Timbavati Private Game Reserve. These scenes were observed nearly simultaneously by the ER-2 and the Terra spacecraft. Panel (c) shows the brightness temperature as a function of wavenumber obtained by the S-HIS over a 2 km pixel near the center of Timbavati fire. The 'blue spike' is a spectral feature associated with the hot fire near 2400 cm^{-1} (4.166 μm).

Plate 5. Brightness temperature of the Okavango Delta, Botswana at 10.2 μm, acquired by Scanning HIS during 6 parallel flight lines over the Delta on August 27, 2000. The pixel resolution of S-HIS is 2 km at nadir.

Plate 6. These MAS images of a prescribed fire and nearby clouds were acquired over the Madikwe Private Game Reserve, South Africa, on August 20, 2000. Panel (a) is a true color RGB composite of bands at

0.66, 0.55, and 0.47 μm, (b) a false color composite of bands at 3.94, 2.18, and 1.67 μm, and (c) the resultant cloud, shadow, and fire mask. All images have been resampled to a constant spatial resolution of 64 m resolution. The thermal emission of the hot fire line clearly shows up beneath the smoke using the shortwave infrared bands.

Plate 7. CPL observations of attenuated backscatter coefficient at 1.064 μm on August 24, 2000 obtained as the ER-2 aircraft flew from the highveld west of Witbank, South Africa, over the escarpment to Inhaca Island, Mozambique and then turned north over nearby Maputo Bay paralleling the Terra ground track. The multiple layers of smoke and haze are clearly evident in this plate.

Plate 8. SSFR observations of spectral downwelling and upwelling irradiance on August 24, 2000 as the ER-2 aircraft flew over coastal Mozambique and Maputo Bay near Inhaca Island. Based on these measurements, the spectral albedo of the underlying surface (plus atmosphere) clearly shows differences between the spectral reflectance of vegetation, which is bright in the near-infrared, and water, which is dark in the near-infrared.

Plate 9. MOPITT-A calibrated average radiance at 4.7 μm in units of W m^{-2} sr^{-1} for the entire ER-2 flight on September 7, 2000. This channel is mainly sensitive to surface or cloud top temperatures beneath the instrument.

Plate 10. RC-10 color infrared photograph of Mongu, Zambia and the nearby Zambezi River to the west of town, acquired on August 25, 2000.

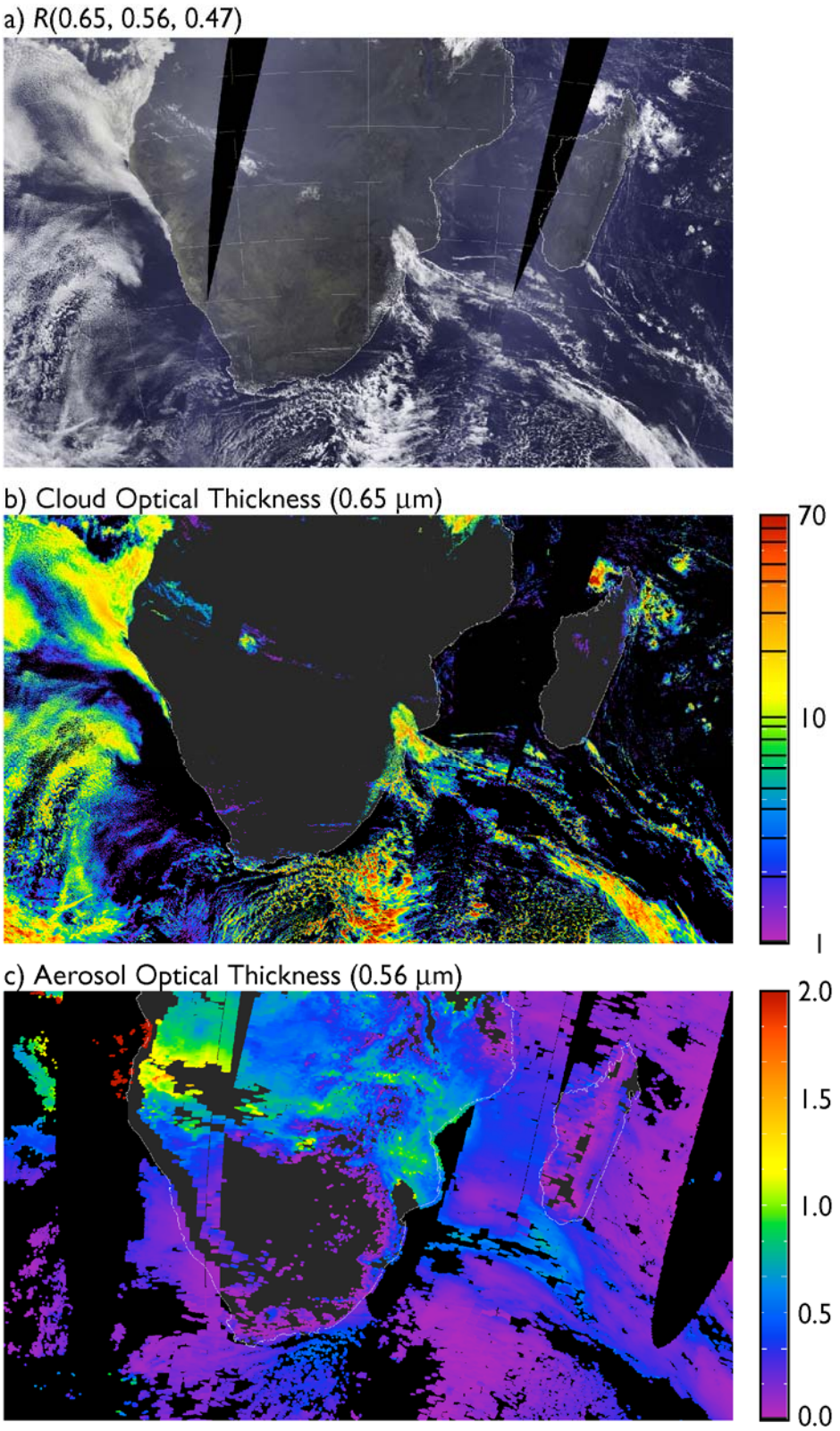

Plate 1. MODIS atmospheric properties over southern Africa on 3 consecutive descending daytime orbits on September 7, 2000. Panel (a) is a true color composite constructed from red (0.65 μm), green (0.56 μm) and blue (0.47 μm) bands. Panel (b) is the cloud optical thickness at 0.65 μm and (c) the aerosol optical thickness at 0.56 μm.

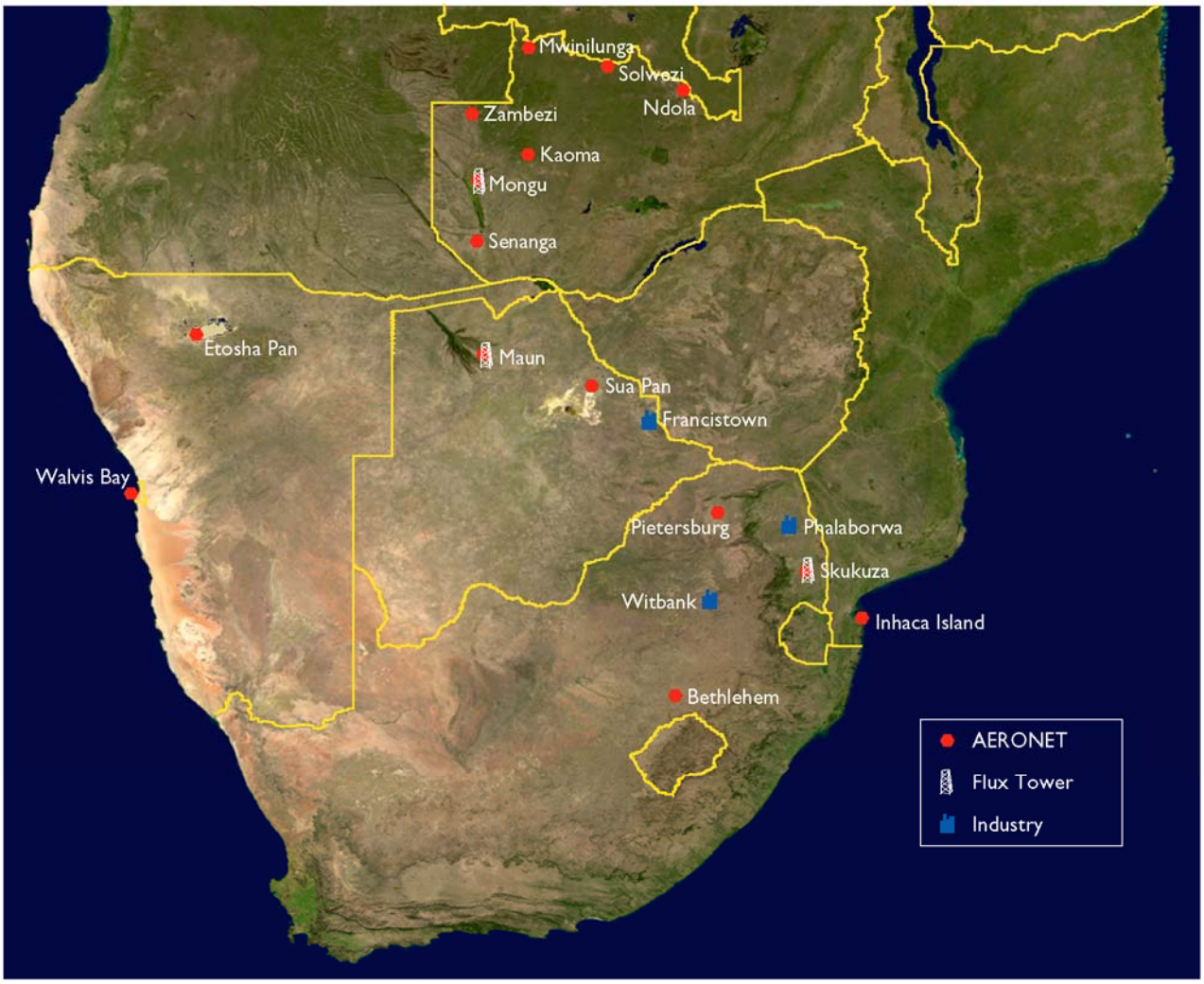

Plate 2. Location of AERONET, Flux Tower, and primary industrial sites throughout southern Africa that were overflown by the NASA ER-2 aircraft during SAFARI 2000.

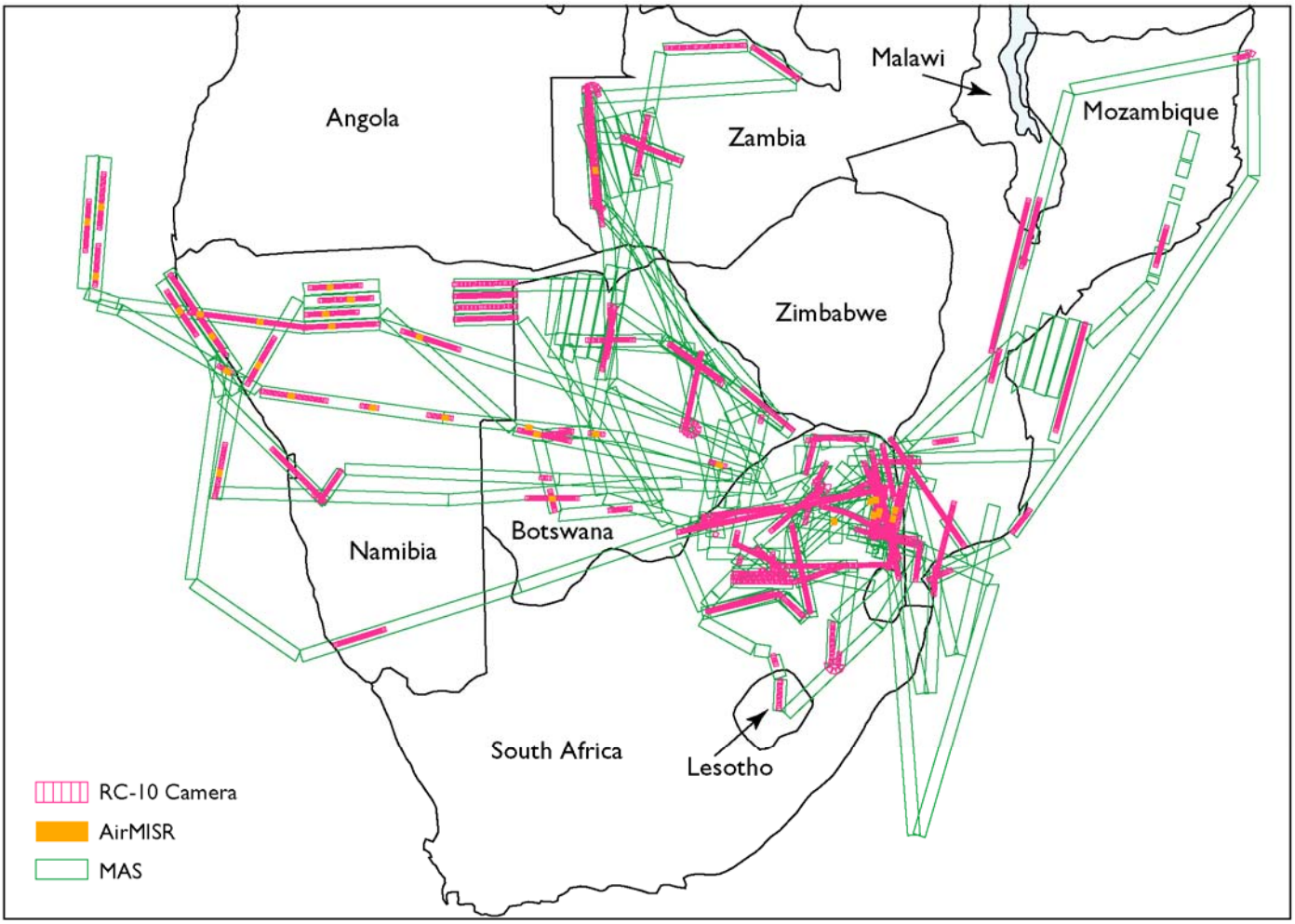

Plate 3. Coverage of the RC-10 camera, AirMISR, and MAS on all ER-2 flights throughout SAFARI 2000.

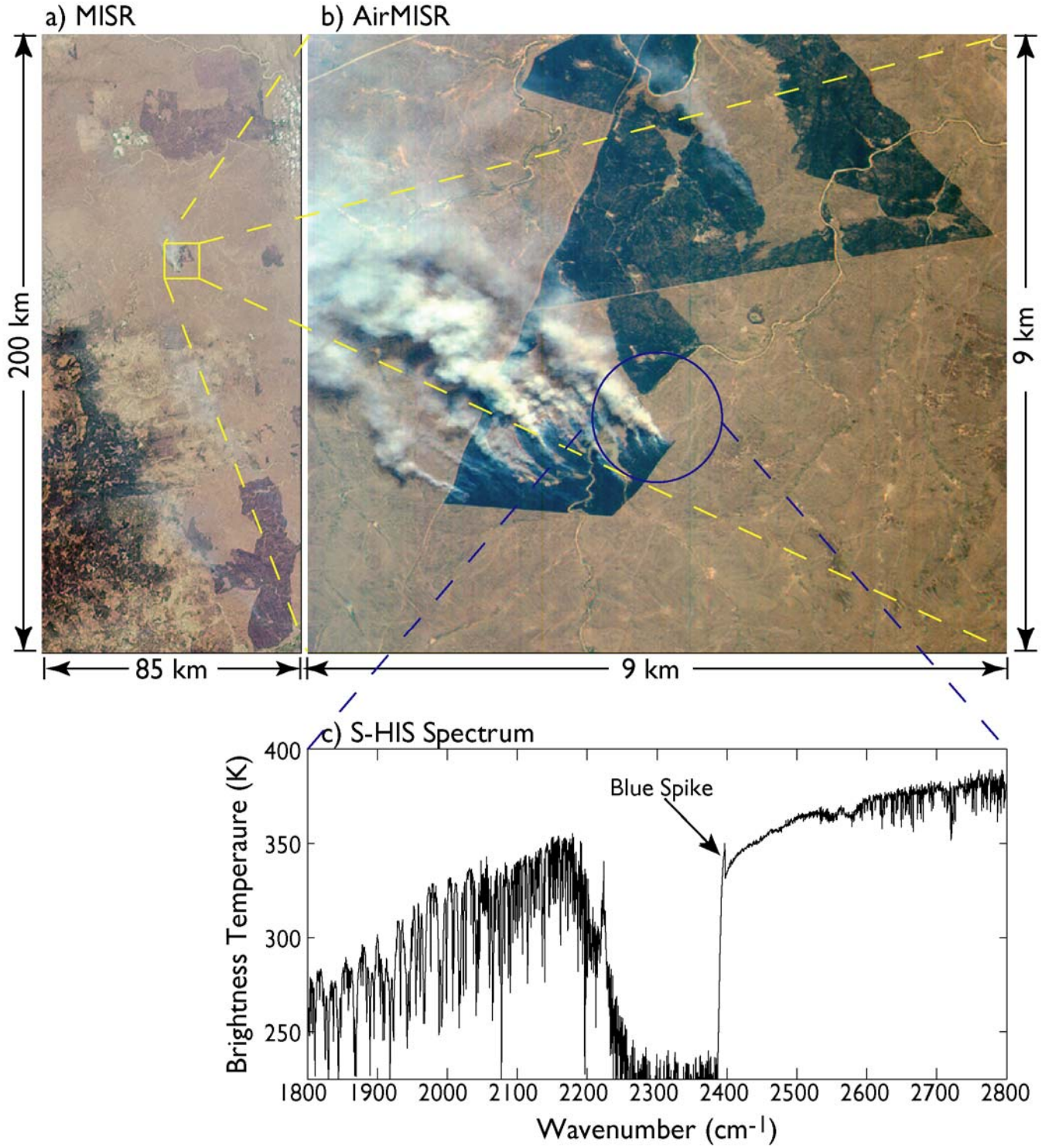

Plate 4. These images of northeastern South Africa were acquired on September 7, 2000 at 0825 UTC by MISR (a) and AirMISR (b). Panel (a) is an 85 x 200 km swath of MISR's aft-viewing 45° camera, and (b) an AirMISR 9 x 9 km nadir-viewing image of the prescribed fire in the Timbavati Private Game Reserve. These scenes were observed nearly simultaneously by the ER-2 and the Terra spacecraft. Panel (c) shows the brightness temperature as a function of wavenumber obtained by the S-HIS over a 2 km pixel near the center of Timbavati fire. The 'blue spike' is a spectral feature asso-ciated with the hot fire near 2400 cm^{-1} (4.166 μm).

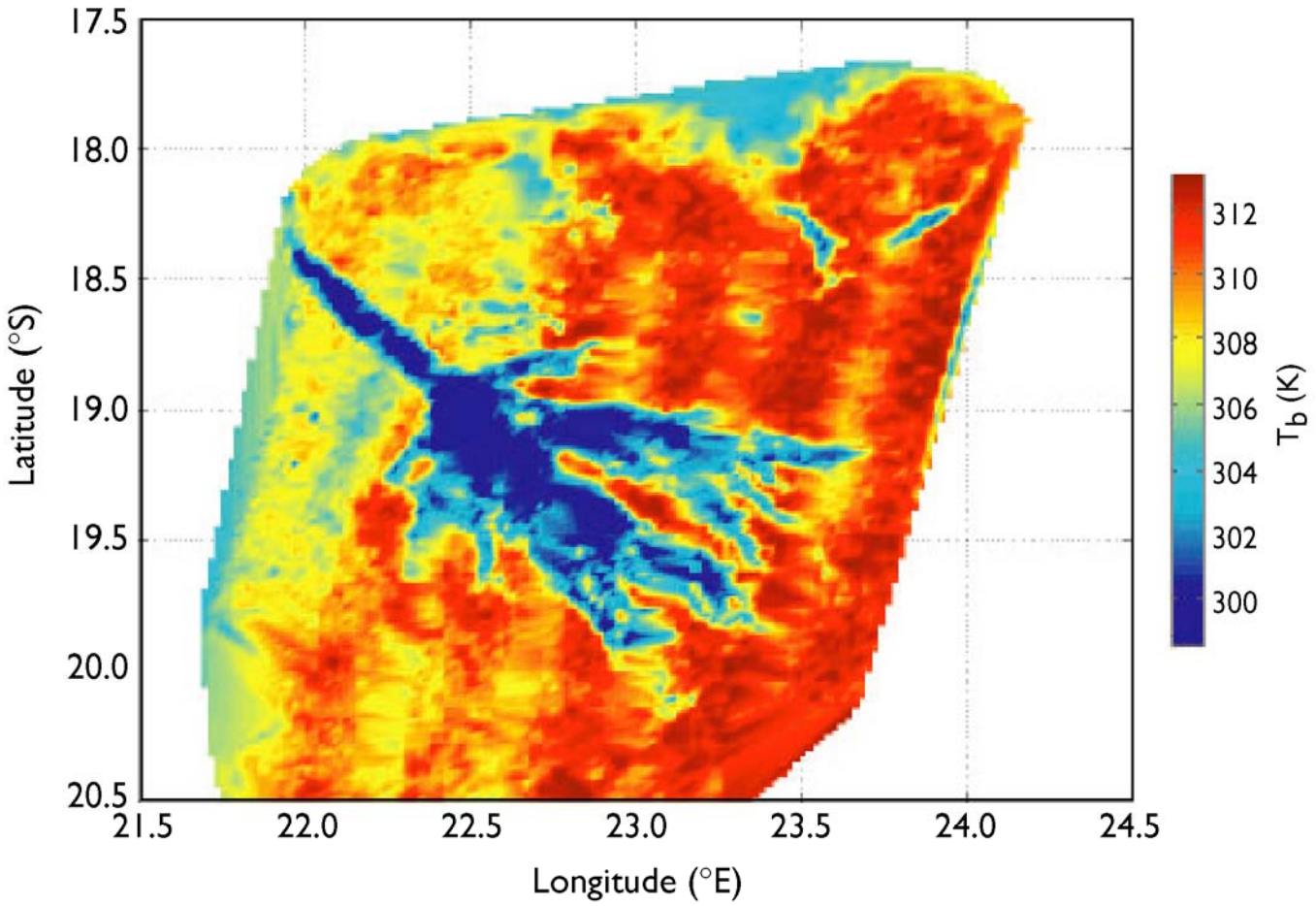

Plate 5. Brightness temperature of the Okavango Delta, Botswana at 10.2 μm, acquired by Scanning HIS during 6 parallel flight lines over the Delta on August 27, 2000. The pixel resolution of S-HIS is 2 km at nadir.

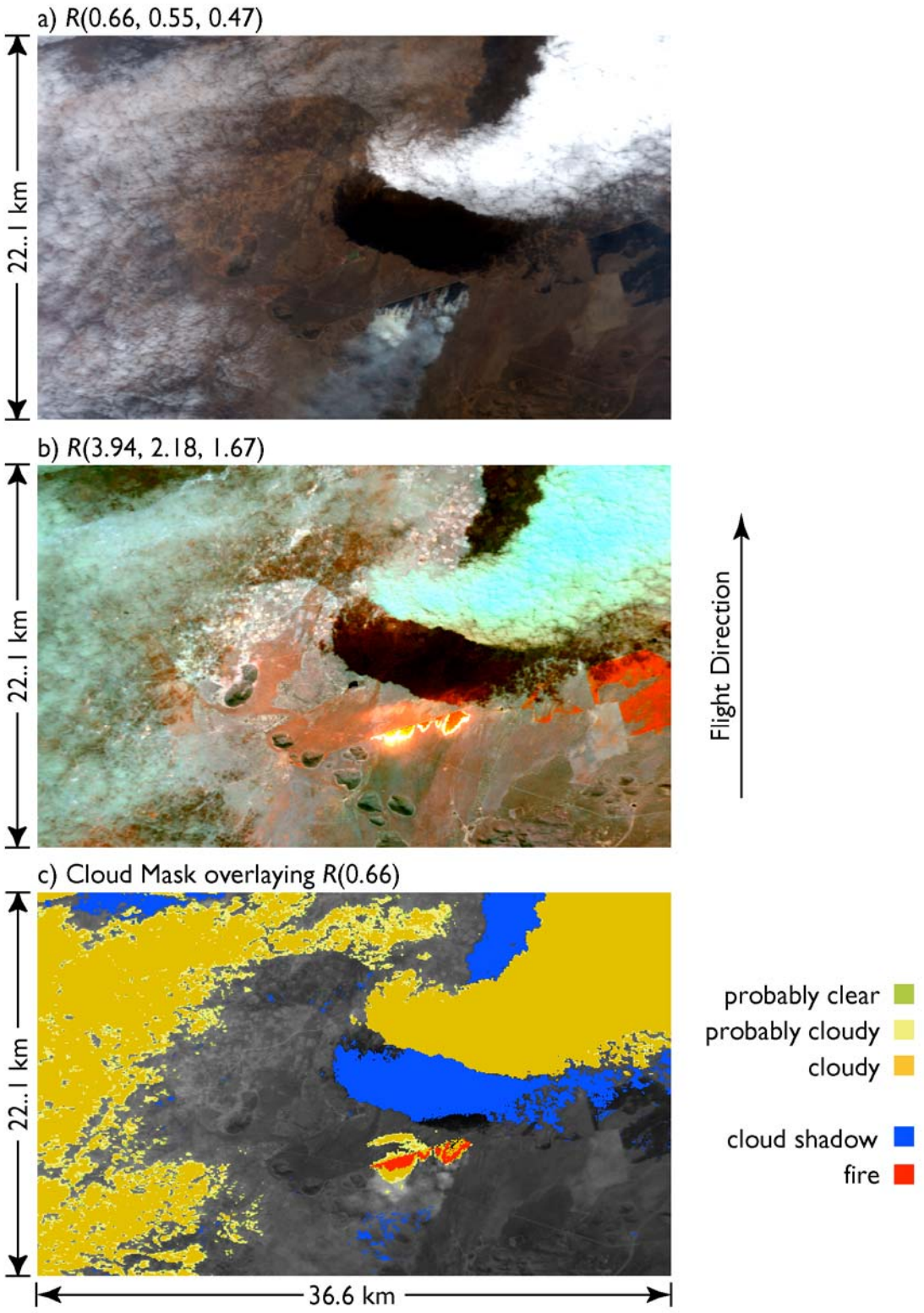

Plate 6. These MAS images of a prescribed fire and nearby clouds were acquired over the Madikwe Private Game Reserve, South Africa, on August 20, 2000. Panel (a) is a true color RGB composite of bands at 0.66, 0.55, and 0.47 μm, (b) a false color composite of bands at 3.94, 2.18, and 1.67 μm, and (c) the resultant cloud, shadow, and fire mask. All images have been resampled to a constant spatial resolution of 64 m resolution. The thermal emission of the hot fire line clearly shows up beneath the smoke using the shortwave infrared bands.

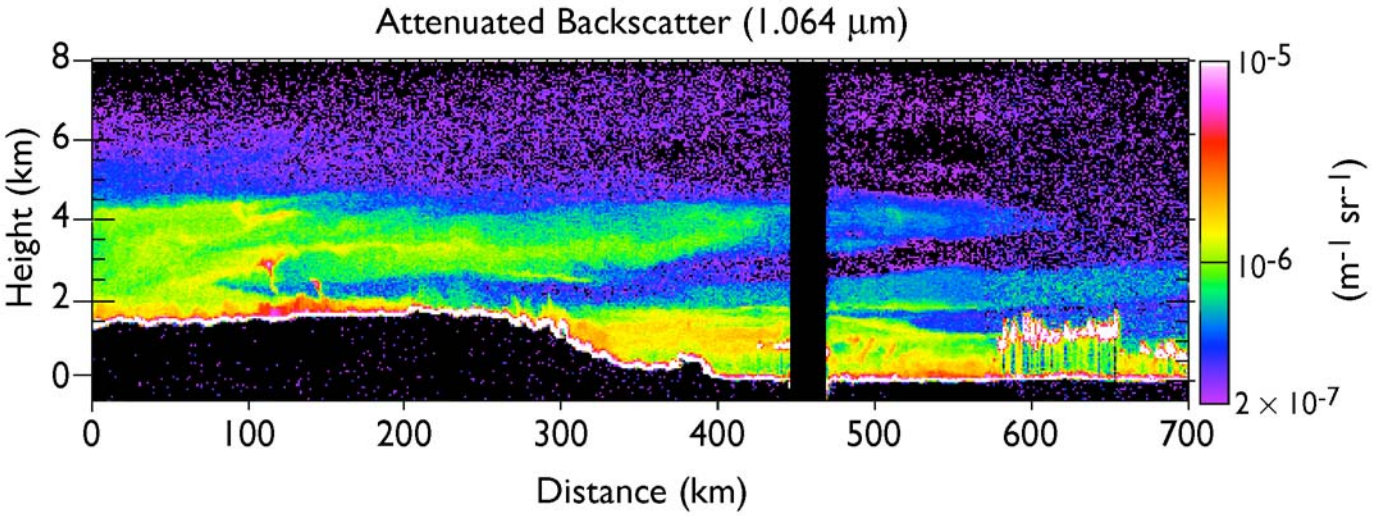

Plate 7. CPL observations of attenuated backscatter coefficient at 1.064 μm on August 24, 2000 obtained as the ER-2 aircraft flew from the highveld west of Witbank, South Africa, over the escarpment to Inhaca Island, Mozambique and then turned north over nearby Maputo Bay parallel-ing the Terra ground track. The multiple layers of smoke and haze are clearly evident in this plate.

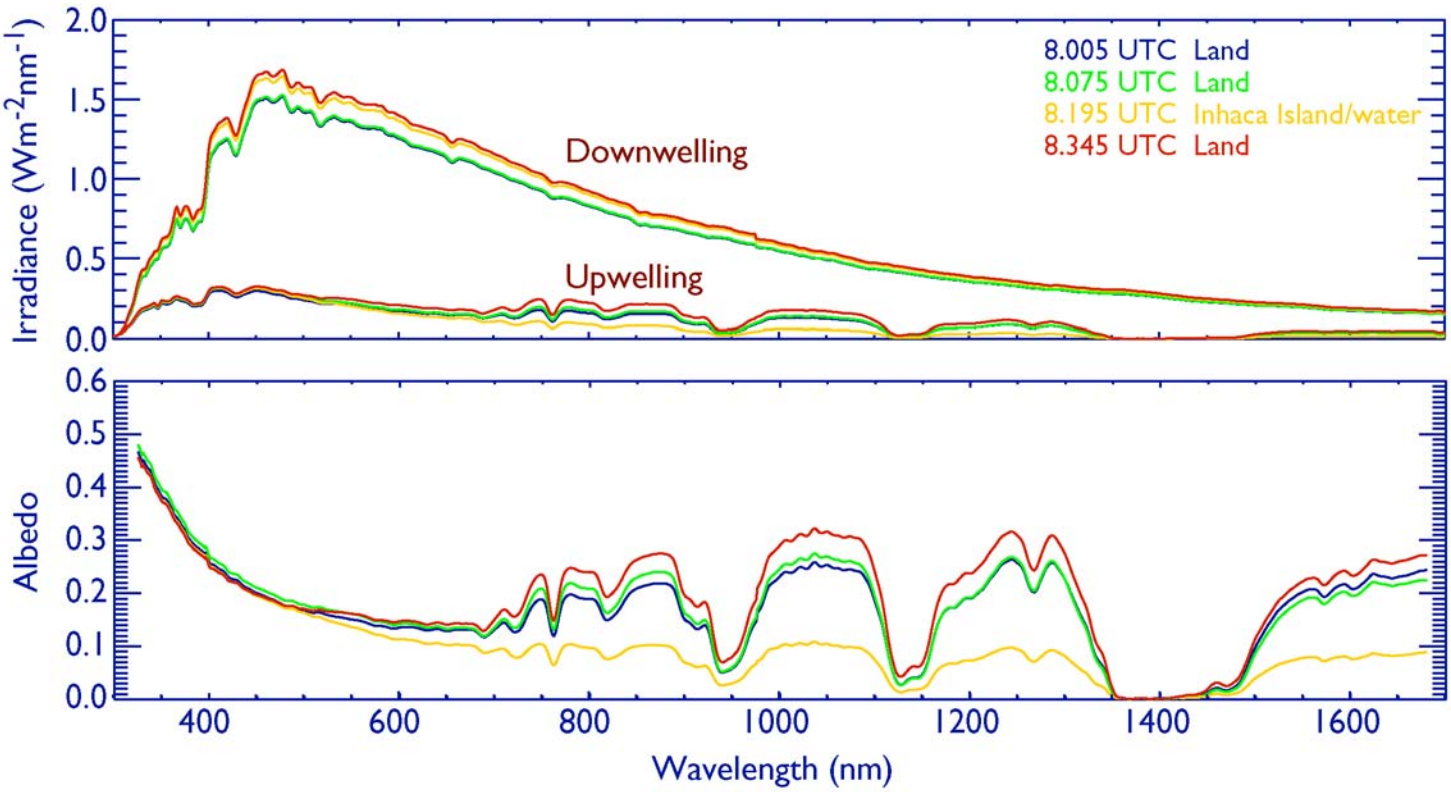

Plate 8. SSFR observations of spectral downwelling and upwelling irradiance on August 24, 2000 as the ER-2 aircraft flew over coastal Mozambique and Maputo Bay near Inhaca Island. Based on these measurements, the spectral albedo of the underlying surface (plus atmosphere) clearly shows differences between the spectral reflectance of vegetation, which is bright in the near-infrared, and water, which is dark in the near-infrared.

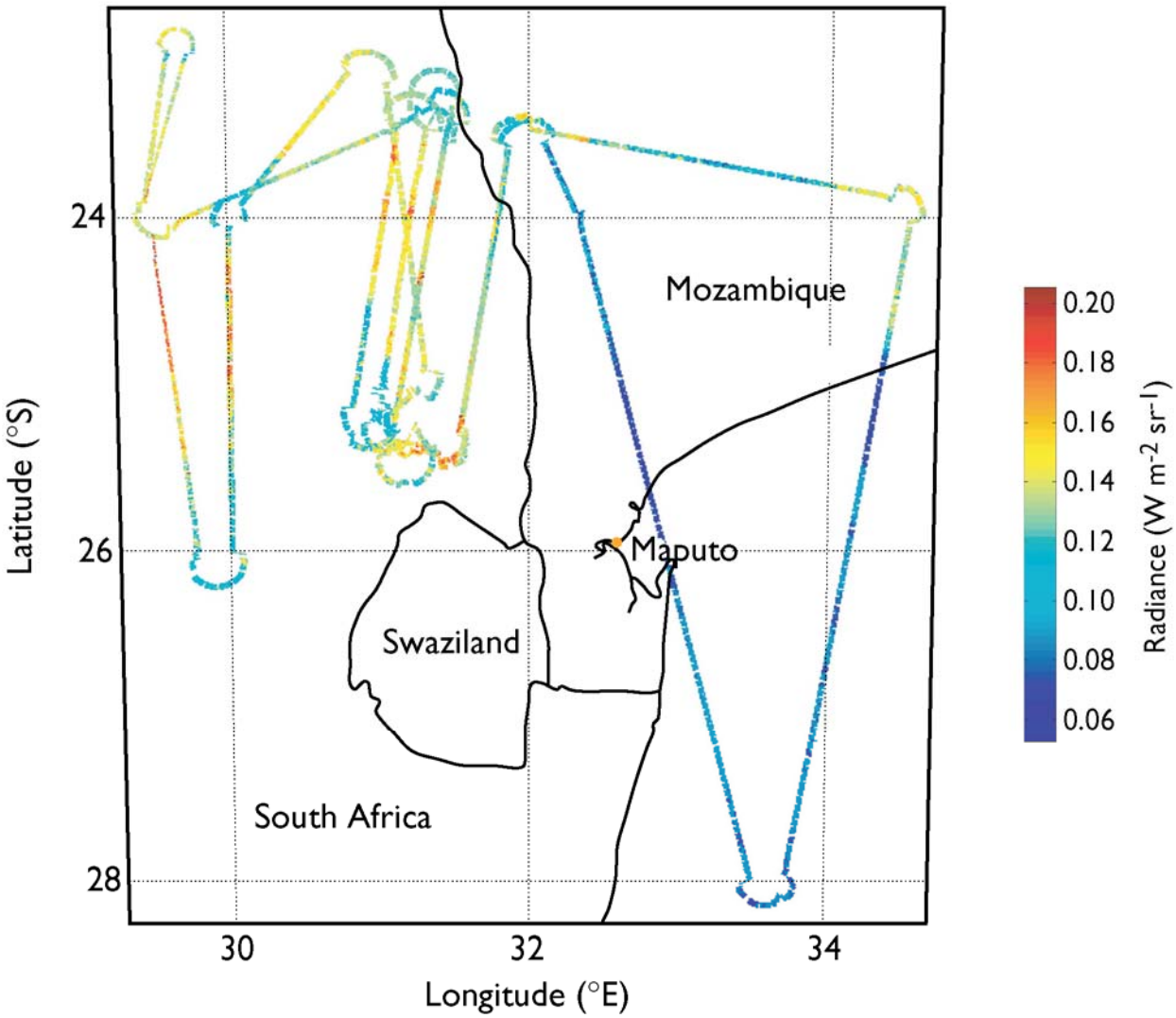

Plate 9. MOPITT-A calibrated average radiance at 4.7 μm in units of W m^{-2} sr^{-1} for the entire ER-2 flight on September 7, 2000. This channel is mainly sensitive to surface or cloud top temperatures beneath the instrument.

Plate 10. RC-10 color infrared photograph of Mongu, Zambia and the nearby Zambezi River to the west of town, acquired on August 25, 2000.